DR ZAMAN ASHRAF (Orcid ID : 0000-0002-6620-9080)

DR AAMER SAEED (Orcid ID : 0000-0002-7112-9296)

Article type : Research Article

Synthesis, enzyme inhibitory kinetics and computational studies of novel 1-(2-(4-isobutylphenyl) propanoyl)-3-arylthioureas as Jack bean urease inhibitors

Tanzeela Abdul Fattah[1], Aamer Saeed[1,*], Pervaiz Ali Channar[1], Zaman Ashraf[2,*], Qamar Abbas[3], Mubashir Hassan[3], Fayaz Ali Larik[1]

[1]*Department of Chemistry Quaid-i-Azam University-45320, Islamabad, Pakistan.*

[2]*Department of Chemistry, Allama Iqbal Open University, Islamabad 44000, Pakistan*

[3]*Department of Biology, College of Natural Sciences, Kongju National University, Gongju 314-701, Republic of Korea*

*** Address for Correspondence**

Aamer Saeed

Email: asaeed@qau.edu.pk, aamersaeed@yahoo.com

Contact number: +92-51-9064-2128, Fax: +92-51-9064-2241

*** Address for Correspondence**

Zaman Ashraf,

Email: mzchem@yahoo.com

Contact number: +923215194461, Fax: +92512891471

This article has been accepted for publication and undergone full peer review but has not been through the copyediting, typesetting, pagination and proofreading process, which may lead to differences between this version and the Version of Record. Please cite this article as doi: 10.1111/cbdd.13090

Abstract

In this article synthesis of a novel 1-(2-(4-isobutylphenyl)propanoyl)-3-arylthioureas (**4a-j)** as jack bean urease inhibitors has been described. Freshly prepared 2-(4-isobutylphenyl) propanoyl isothiocyanate was treated with substituted aromatic anilines in one pot using anhydrous acetone. The compounds **4e, 4h** and **4j** showed IC_{50} values 0.0086nM, 0.0081nM and 0.0094nM respectively. The enzyme inhibitory kinetics results showed that compound **4h** inhibit the enzyme competitively while derivatives **4e** and **4j** are the mixed type inhibitors. The compound **4h** reversibly binds the urease enzyme showing *Ki* value 0.0012nM. The *Ki* values for **4e** and **4j** are 0.0025nM and 0.003nM respectively. The antioxidant activity results reflected that compounds **4b, 4i** and **4j** showed excellent radical scavenging activity. Moreover, the cytotoxic activity of the target compounds was evaluated using brine shrimp assay and it was found that all of the synthesized compounds exhibited no cytotoxic effects to brine shrimps. The computational molecular docking and molecular dynamic simulation of title compounds was also performed and results showed that the wet lab findings are in good agreement to the dry lab results. Based upon our results it is proposed that compound **4h** may act as a lead candidate to design the clinically useful urease inhibitors.

Keywords: Thioureas, Synthesis, Jack bean urease, Enzyme kinetics, Computaional studies

Introduction

Ureases belongs to a family of large heteropolymeric enzymes having an active site containing two Ni (II) atoms, largely found in Jack bean, soybeans, bacteria, fungi and other plant seeds. They are also present in some animal tissues and intestinal micro-organisms. Ureases catalyzes the hydrolysis of urea, forming ammonia and carbon dioxide which results in the deficiency of nitrogen in the soil and the toxicity of excess ammonia makes soil infertile for crops. It has been reported that ureases are responsible for dangerous factors which include pyelonephritis, hepatic coma, peptic ulceration, stomach cancer and injection-induced urinary stones (1-2). Besides human health ureases have a detrimental impact on the economic impact for farmers due to excessive loss of ammonia from fertilizers. In addition, interference of this ammonia to the atmosphere will consequently be deposited to land or

water which results in eutrophication and acidification of natural ecosystems on a regional scale (3). Thus the development of new and effective urease inhibitors is a crucial task not only for the treatment of human diseases but also to control the eutrophication and acidification of natural ecosystems.

Ibuprofen is [2-(4-isobutylphenyl) propanoic acid], commercially available as "Advil or Motrin" and is a well known nonsteroidal anti-inflammatory drug (NSAID) used for the treatment of rheumatism and arthritis. The drug relieves pain and swelling by inhibiting the formation of prostaglandins which are flat-like molecules derived from arachidonic acid. Ibuprofen is a classical NSAID, it inhibits cyclooxygenase enzyme and it's both isoforms COX-1 and COX-2, involved in first step of the arachidonic acid cascade. But it produces increased risk of side effects such as, gastrointestinal hemorrhage, ulceration, decreased renal function, bleeding and perforation (4-7). NSAIDs side effects are believed to be involved by two different mechanisms: a local action exerted by direct contact of drug with gastric mucosa and generalized systemic action following absorption that is believed to be inhibition of COX-1 (8-11). These side effects are thought to be due to free –COOH group of NSAIDs, therefore safer and effective derivatives of NSAIDs are prepared to minimize their side effects (12). Many derivatives of ibuprofen have been prepared such as, sugar, amide, ester and hydrazone derivatives which show anti-inflammatory activity comparable with that of parent drug but minimum gastrotoxicity. Thus masking of free carboxylic group is the principal of reduced topical irritant action (13).

During the couple of decades, tremendous research focus has been devoted on the preparation, characterization and functional studies of thiourea derivatives. 1,3-Disubstituted thioureas are valuable building blocks for generating a variety of heterocyclic compounds. *N*,*N*-Dialkyl-*N*-aroylthioureas are selective reagents for separation of platinum group metals (14). Thiocarbonyl group containing compounds (thioureas) show higher efficiency in inhibiting corrosion, and due to this property thiourea is an industrially significant molecule, and has been widely used as an electroplating additive, corrosion inhibitor, rubber accelerator, and for extracting precious metals (15). 1,3-Dibenzylthiourea (DBTU) has been investigated as carbon steel corrosion inhibitor (16). Thioureas have found extensive applications in the field of medicine, agriculture, analytical and coordination chemistry (17a-17b) and are used as chelating agents (18). Various biological activities have been reported for thioureas such as, antifungal, herbicidal, antitubercular, antifungal and insecticidal (19-

20). Thiourea derivatives of amlodipine possess antimicrobial activities (21), whereas thiourea derivatives of bisindolylmethane act as carbonic anhydrase (II) inhibitors (22). Zhang reported thiourea-appended 1,8-naphthalimide as chemosensor for detection of heavy metal ions (23), and *N*-(4-Aminophenylethynylbenzonitrile)-*N*′-(1-naphthoyl)thiourea act as chemosensor for carbon monoxide sensing (24). Ethoxy carbonyl thiourea is used as collector for improving copper flotation recovery from copper porphyry ore (25). 1-Aroyl-3-arylthioureas have been used in the synthesis of imidazole-2-thiones (26) and 1,3-thiazolines (27). In this article some new ibuprofenyl-arylthioureas (**4a-j)** were synthesized and evaluated for their Jack Bean Urease inhibitory potential, antioxidant and cytotoxic activities.

Experimental

Methods and materials

The chemicals, thionyl chloride, ibuprofen, 2,4-dinitroaniline, 4-bromoaniline, p-anisidine, 3,5-dinitroaniline, 3-nitroaniline, 4-chloroaniline, 4-aminobenzenesulfonamide, 2,3-dichloroaniline, 2,4,6-trimethylaniline, benzyl amine, phenylmethanamine, all synthetic starting materials, reagents and solvents were of analytical reagent grade or of the highest quality commercially available and were purchased from Sigma Aldrich Chemical Co., Merck Germany and was used without further purification. Acetone was freshly dried over $KMnO_4$ and distilled. R_f-values were determined using pre-coated silica gel aluminum plates $60F_{254}$ from Merck (Germany). Melting points were determined in an open glass capillaries using Gallenkamp melting point apparatus (MP-D) and are uncorrected. Infrared spectra (IR) of the compounds were recorded on a Bio-Rad-Excalibur Series Model No.FTS 300 MX spectrophotometer as pure compounds. ^{1}H and ^{13}C-NMR spectra were obtained on a Bruker 300 MHz and 75.5 MHz NMR spectrometer using teteramethyl silane (TMS) as internal reference standard. Elemental analyses were conducted using a LECO-183 CHNS analyser.

Procedure for the synthesis of 2-(4-isobutylphenyl)propanoyl chloride (2)

A solution of 2-(4-isobutylphenyl)propanoic acid **1** (1.0 mmol, 0.2 g) and DMF (0.05 mL) in thionyl chloride (1.2 mmol) was refluxed for 3 h. After cooling at room temperature, the mixture was concentrated in *vacuo* to afford 2-(4-isobutylphenyl)propanoyl chloride (**2**).

Synthesis of 1-(2-(4-isobutylphenyl) propanoyl)-3-arylthioureas (4a-j)

A solution of 2-(4-isobutylphenyl)propanoyl chloride **2** (1.0 mmol) in dry distilled acetone (20 mL) was added drop wise to a suspension of potassium thiocyanate (1.0 mmol) in dry acetone and refluxed for 1.5 h at 50ºC. After cooling on room temperature a solution of substituted aromatic aniline (1.0 mmol) in acetone was added and the mixture was refluxed for 7-8 h. The progress of the reaction was monitored by TLC, EtOAc : n-hexane (1:2). After the reaction was completed it was poured onto crushed ice and the precipitates were collected by filtration, washed, dried and recrystallized from ethanol to yield the 1-(2-(4-isobutylphenyl)propanoyl)-3-arylthiourea derivatives (**4a-j)**.

1-(3,5-Dinitrophenyl)-3-(2-(4-isobutylphenyl)propanoyl)thiourea (4a)

Light brown solid; yield: 78%; m.p: 163^{o}C; R_f: 0.5 (n-Hexane : Ethyl acetate 1:1); IR (KBr) cm^{1}: 3371, 3223 (N-H), 3024, 2934 (C_{sp2}-H), 2878 (C_{sp3}–H), 1682 (C=O), 1615, 1595 (C=C Ar), 1259 (C=S); ^{1}H NMR (300 MHz, DMSO-*d*$_6$): δ (ppm) 12.43 (1H, s, broad, NH), 8.69 (1H, s, broad, NH), 7.31-7.55 (d, 2H, *J* = 8.1 Hz, Ar-H), 7.11-7.23 (d, 2H, *J* = 8.1 Hz, Ar-H), 8.55 (t, 1H, *J* = 7.6 Hz, Ar-H), 7.85 (d, 2H, *J* = 7.6 Hz, Ar-H), 4.62 (q, 1H, *J* = 7.10 Hz, $CHCH_3$), 2.41 (d, 2H, *J* = 7.17 Hz, $(CH_3)_2CHCH_2Ar$), 1.82 (m, 1H, $CH(CH_3)_2$), 1.40 (d, 3H, *J* = 7.3 Hz, $ArCHCH_3$), 0.86 (d, 6H, J = 6.56 Hz, $CH(CH_3)_2$); ^{13}C NMR (75.5 MHz, DMSO-*d*$_6$); 178.6 (C=S), 174.5 (C=O), 149.2, 141.9, 140.5, 134.9, 133.5, 129.6, 128.2, 120.5 (Ar-Cs), 44.5, 42.5, 31.1, 22.9, 18.2 Anal. Calcd. for $C_{20}H_{22}N_4O_5S$: C, 55.80; H, 5.15; N, 13.02; S, 7.45 found: C, 55.78; H, 5.13; N, 13.00; S, 7.43.

1-(4-Bromophenyl)-3-(2-(4-isobutylphenyl)propanoyl)thiourea (4b)

Brown solid; yield: 69%; m.p: 174^{o}C; R_f: 0.7 (n-Hexane : Ethyl acetate 1:1); IR (KBr) cm^{1}: 3288, 3211 (N-H), 3032, 2945 (C_{sp2}-H), 2812 (C_{sp3}–H), 1686 (C=O), 1565, 1467 (C=C Ar), 1260 (C=S); ^{1}H NMR (300 MHz, DMSO-*d*$_6$): δ (ppm) 13.53 (1H, s, broad, NH), 9.76 (1H, s, broad, NH), 7.21-7.39 (d, 2H, *J* = 8.2 Hz, Ar-H), 7.11-7.20 (d, 2H, *J* = 8.2 Hz, Ar-H), 7.29 (d, 2H, *J* = 7.55 Hz, Ar-H), 6.49 (d, 2H, *J* = 7.55 Hz, Ar-H), 3.79 (q, 1H, *J* = 7.11 Hz, $CHCH_3$), 2.52 (d, 2H, *J* = 7.13 Hz, $(CH_3)_2CHCH_2Ar$), 1.85 (m, 1H, $CH(CH_3)_2$), 1.56 (d, 3H, *J* = 7.1 Hz, $ArCHCH_3$), 0.91 (d, 6H, *J* = 6.51 Hz, $CH(CH_3)_2$); ^{13}C NMR (75.5 MHz, DMSO-*d*$_6$); 184.3 (C=S), 176.4 (C=O), 140.5, 138.5, 133.7, 133.1, 129.1, 128.9, 127.5, 119.2 (Ar-

Cs), 46.2, 44.5, 28.7, 22.5, 18.3 Anal. Calcd. for $C_{20}H_{23}BrN_2OS$: C, 57.28; H, 5.53; N, 6.68; S, 3.82 found: C, 57.20; H, 5.51; N, 6.66; S, 3.80.

1-(2-(4-isobutylphenyl)propanoyl)-3-(4-methoxyphenyl)thiourea (4c)

Yellow solid; yield: 82%; m.p: 186°C; R_f: 0.7 (n-Hexane : Ethyl acetate 2:1); IR (KBr) cm^1: 3321, 3211 (N-H), 3076, 2945 (C_{sp2}-H), 2814 (C_{sp3}–H), 1684 (C=O), 1594, 1445 (C=C Ar), 1278 (C-O-C), 1258 (C=S); ^{1}H NMR (300 MHz, DMSO-d_6): δ (ppm) 12.99 (1H, s, broad, NH), 8.87 (1H, s, broad, NH), 7.33-7.45 (d, 2H, *J* = 8.2 Hz, Ar-H), 7.21-7.29 (d, 2H, *J* = 8.2 Hz, Ar-H), 6.60 (m, 2H, Ar-H), 6.49 (m, 2H, Ar-H), 3.88 (q, 1H, *J* = 7.10 Hz, $CHCH_3$), 3.65 (s, 3H, OCH_3), 2.59 (d, 2H, *J* = 7.12 Hz, $(CH_3)_2CHCH_2Ar$), 1.83 (m, 1H, $CH(CH_3)_2$), 1.55 (d, 3H, *J* = 7.2 Hz, $ArCHCH_3$), 0.95 (d, 6H, *J* = 6.52 Hz, $CH(CH_3)_2$); ^{13}C NMR (75.5 MHz, DMSO-d_6); 180.6 (C=S), 173.5 (C=O), 155.8, 138.3, 134.1, 129.5, 129.4, 128.9, 127.1, 114.3 (Ar-Cs), 54.7, 45.2, 40.4, 31.5, 25.3, 18.2 Anal. Calcd. for $C_{21}H_{26}N_2O_2S$: C, 68.08; H, 7.07; N, 7.56; S, 8.65 found: C, 68.06; H, 7.05; N, 7.54; S, 8.63.

1-(2,4-Dinitrophenyl)-3-(2-(4-isobutylphenyl)propanoyl)thiourea (4d)

Pale Yellow solid; yield: 84%; m.p: 168-169°C; R_f: 0.64 (n-Hexane : Ethyl acetate 2:1); IR (KBr) cm^1: 3345, 3212 (N-H), 3023, 2932 (C_{sp2}-H), 2838 (C_{sp3}–H), 1690 (C=O), 1525, 1450 (C=C Ar), 1265 (C=S); ^{1}H NMR (300 MHz, DMSO-d_6): δ (ppm) 12.38 (1H, s, broad, NH), 9.12 (1H, s, broad, NH), 7.23-7.34 (d, 2H, *J* = 8.2 Hz, Ar-H), 7.12-7.20 (d, 2H, *J* = 8.2 Hz, Ar-H), 8.95 (s, 1H, Ar-H), 8.35 (d, 1H, *J* = 8.35 Hz, Ar-H), 7.18 (d, 1H, *J* = 8.35 Hz, Ar-H), 4.10 (q, 1H, *J* = 7.10 Hz, $CHCH_3$), 2.49 (d, 2H, *J* = 7.13 Hz, $(CH_3)_2CHCH_2Ar$), 1.86 (m, 1H, $CH(CH_3)_2$), 1.59 (d, 3H, *J* = 7.3 Hz, $ArCHCH_3$), 0.93 (d, 6H, *J* = 6.54 Hz, $CH(CH_3)_2$); ^{13}C NMR (75.5 MHz, DMSO-d_6); 186.3 (C=S), 179.2 (C=O), 145.2, 144.3, 140.6, 140.1, 128.8, 128, 127.8, 120.1 (Ar-Cs), 44.1, 40.2, 31.7, 21.7, 18.5 Anal. Calcd. for $C_{20}H_{22}N_4O_5S$: C, 55.80; H, 5.15; N, 13.02; S, 7.45 found: C, 55.78; H, 5.13; N, 13.00; S, 7.41.

1-(2-(4-isobutylphenyl)propanoyl)-3-(3-nitrophenyl)thiourea (4e)

Reddish brown solid; yield: 73%; m.p: 179°C; R_f: 0.76 (n-Hexane : Ethyl acetate 2:1); IR (KBr) cm^1: 3323, 3219 (N-H), 3123, 2935 (C_{sp2}-H), 2874 (C_{sp3}–H), 1680 (C=O), 1555, 1489 (C=C Ar), 1255 (C=S); ^{1}H NMR (300 MHz, DMSO-d_6): δ (ppm) 13.12 (1H, s, broad, NH),

9.39 (1H, s, broad, NH), 7.30-7.45 (d, 2H, *J* = 8.0 Hz, Ar-H), 7.21-7.29 (d, 2H, *J* = 8.0 Hz, Ar-H), 7.76 (m, 1H, Ar-H), 7.40 (s, 1H, Ar-H), 7.15 (m, 1H, Ar-H), 6.83 (m, 1H, Ar-H), 3.92 (q, 1H, *J* = 7.10 Hz, $CHCH_3$), 2.61 (d, 2H, *J* = 7.16 Hz, $(CH_3)_2CHCH_2Ar$), 1.85 (m, 1H, $CH(CH_3)_2$), 1.49 (d, 3H, *J* = 7.2 Hz, $ArCHCH_3$), 0.88 (d, 6H, *J* = 6.54 Hz, $CH(CH_3)_2$); ^{13}C NMR (75.5 MHz, DMSO-*d*$_6$); 180.6 (C=S), 176.4 (C=O), 149.2, 140.1, 137.3, 134.2, 133.2, 130.6, 130.1, 128.5, 121.5, 118.5 (Ar-Cs), 43.2, 40.5, 32.5, 24.7, 17.6 Anal. Calcd. for $C_{20}H_{23}N_3O_3S$: C, 62.32; H, 6.01; N, 10.90; S, 8.32 found: C, 62.30; H, 5.98; N, 10.88; S, 8.30.

1-(4-Chlorophenyl)-3-(2-(4-isobutylphenyl)propanoyl)thiourea (4f)

Light brown solid; yield: 56%; m.p: 175^{o}C; R_f: 0.56 (n-Hexane : Ethyl acetate 1:1); IR (KBr) cm^1: 3312, 3267 (N-H), 3121, 2937 (C_{sp2}-H), 2865 (C_{sp3}–H), 1683 (C=O), 1576, 1496 (C=C Ar), 1250 (C=S), 754 (C-Cl); ^1H NMR (300 MHz, DMSO-*d*$_6$): δ (ppm) 12.99 (1H, s, broad, NH), 8.78 (1H, s, broad, NH), 7.55-7.60 (d, 2H, *J* = 8.1 Hz, Ar-H), 7.29-7.35 (d, 2H, *J* = 8.1 Hz, Ar-H), 7.13 (d, 2H, *J* = 8.4 Hz, Ar-H), 6.63 (d, 2H, *J* = 8.4 Hz, Ar-H), 3.99 (q, 1H, *J* = 7.11 Hz, $CHCH_3$), 2.87 (d, 2H, *J* = 7.15 Hz, $(CH_3)_2CHCH_2Ar$), 1.88 (m, 1H, $CH(CH_3)_2$), 1.56 (d, 3H, *J* = 7.1 Hz, $ArCHCH_3$), 0.80 (d, 6H, *J* = 6.53 Hz, $CH(CH_3)_2$); ^{13}C NMR (75.5 MHz, DMSO-*d*$_6$); 185.3 (C=S), 179.2 (C=O), 140.3, 136.2, 134.9, 131.2, 130.5, 130.1, 129.2, 128.8 (Ar-Cs), 44.3, 41.5, 33.5, 27.1, 19.2 Anal. Calcd. for $C_{20}H_{23}ClN_2OS$: C, 64.07; H, 6.18; N, 7.47; S, 8.55 found: C, 64.05; H, 6.16; N, 7.45; S, 8.52.

***N*-((4-Sulfamoylphenyl) carbamothioyl-2-(4-isobutylphenyl)propanamide (4g)**

Dark brown solid; yield: 78%; m.p: 179^{o}C; R_f: 0.51 (n-Hexane : Ethyl acetate 1:1); IR (KBr) cm^1: 3253, 3277 (N-H), 3150, 3012 (C_{sp2}-H), 2950 (C_{sp3}–H), 1663 (C=O), 1562, 1545 (C=C Ar), 1263 (C=S), 1136 (C-N); ^1H NMR (300 MHz, DMSO-*d*$_6$): δ (ppm) 12.17 (1H, s, broad, NH), 9.65 (1H, s, broad, NH), 7.98 (d, 2H, *J* = 9.2 Hz, Ar-H), 7.44 (d, 2H, *J* = 9.2 Hz, Ar-H), 7.39-7.55 (d, 2H, *J* = 8.1 Hz, Ar-H), 7.27-7.32 (d, 2H, *J* = 8.1 Hz, Ar-H), 7.09 (s, 2H, SO_2NH_2) 3.76 (q, 1H, *J* = 7.12 Hz, $CHCH_3$), 2.71 (d, 2H, *J* = 7.14 Hz, $(CH_3)_2CHCH_2Ar$), 1.92 (m, 1H, $CH(CH_3)_2$), 1.60 (d, 3H, *J* = 7.1 Hz, $ArCHCH_3$), 0.93 (d, 6H, *J* = 6.54 Hz, $CH(CH_3)_2$); ^{13}C NMR (75.5 MHz, DMSO-*d*$_6$); 186.2 (C=S), 179.2 (C=O), 141.5, 140.1, 139.5, 137.7, 128.2, 127.3, 126.9, 122.5 (Ar-Cs), 46.1, 43.4, 30.5, 22.3, 19.2 Anal. Calcd. for

$C_{20}H_{25}N_3O_3S_2$: C, 57.25; H, 6.01; N, 10.02; S, 15.29 found: C, 57.20; H, 5.98; N, 10.00; S, 15.27.

1-(2,3-Dichlorophenyl)-3-(2-(4-isobutylphenyl)propanoyl)thiourea (4h)

Off white solid; yield: 71%; m.p: 177°C; R_f: 0.55 (n-Hexane : Ethyl acetate 1:1); IR (KBr) cm^1: 3366, 3257 (N-H), 3176, 2954 (C_{sp2}-H), 2812 (C_{sp3}–H), 1681 (C=O), 1554, 1443 (C=C Ar), 1247 (C=S), 732 (C-Cl); ^{1}H NMR (300 MHz, DMSO-d_6): δ (ppm) 13.21 (1H, s, broad, NH), 9.32 (1H, s, broad, NH), 7. 21-7.34 (d, 2H, *J* = 8.2 Hz, Ar-H), 7.01-7.17 (d, 2H, *J* = 8.2 Hz, Ar-H), 6.30-6.66 (m, 3H, Ar-H), 3.96 (q, 1H, *J* = 7.1 Hz, $CHCH_3$), 2.56 (d, 2H, *J* = 7.1 Hz, $(CH_3)_2CHCH_2Ar$), 1.95 (m, 1H, $CH(CH_3)_2$), 1.54 (d, 3H, *J* = 7.2 Hz, $ArCHCH_3$), 0.96 (d, 6H, *J* = 6.9 Hz, $CH(CH_3)_2$); ^{13}C NMR (75.5 MHz, DMSO-d_6); 182.6 (C=S), 177.3 (C=O), 140.1, 138.6, 137.2, 134.5, 134.2, 130.6, 128.8, 128.1, 127.5, 126.3 (Ar-Cs), 46.2, 43.4, 30.3, 26.1, 18.3 Anal. Calcd. for $C_{20}H_{22}Cl_2N_2OS$: C, 58.68; H, 5.42; N, 6.84; S, 7.83 found: C, 58.66; H, 5.40; N, 6.82; S, 7.81.

1-Benzyl-3-(2-(4-isobutylphenyl)propanoyl)thiourea (4i)

Dark brown solid; yield: 66%; m.p: 189°C; R_f: 0.67 (n-Hexane : Ethyl acetate 1:1); IR (KBr) cm^1: 3301, 3224 (N-H), 3112, 2945 (C_{sp2}-H), 2813 (C_{sp3}–H), 1680 (C=O), 1612, 1523 (C=C Ar), 1240 (C=S); ^{1}H NMR (300 MHz, DMSO-d_6): δ (ppm) 12.33 (1H, s, broad, NH), 9.56 (1H, s, broad, NH), 7.12-7.35 (d, 2H, *J* = 8.2 Hz, Ar-H), 7.11-7.31 (d, 2H, *J* = 8.2 Hz, Ar-H), 7.15-7.28 (m, 5H, Ar-H), 3.88 (q, 1H, *J* = 7.2 Hz, $CHCH_3$), 2.61 (d, 2H, *J* = 7.1 Hz, $(CH_3)_2CHCH_2Ar$), 1.92 (m, 1H, $CH(CH_3)_2$), 1.56 (d, 3H, *J* = 7.2 Hz, $ArCHCH_3$), 0.93 (d, 6H, *J* = 6.8 Hz, $CH(CH_3)_2$); ^{13}C NMR (75.5 MHz, DMSO-d_6); 180.6 (C=S), 176.2 (C=O), 142.6, 140.3, 134.6, 130.1, 128.6, 128.1, 127.9, 125.3 (Ar-Cs), 44.2, 40.3, 32.6, 27.2, 18.9 Anal. Calcd. for $C_{21}H_{26}N_2OS$: C, 71.15; H, 7.39; N, 7.90; S, 9.04 found: C, 71.13; H, 7.37; N, 7.88; S, 9.01.

1-(2-(4-isobutylphenyl)propanoyl)-3-mesitylthiourea (4j)

Yellow solid; yield: 76%; m.p: 177°C; R_f: 0.75 (n-Hexane : Ethyl acetate 1:1); IR (KBr) cm^1: 3388, 3260 (N-H), 3080, 2922 (C_{sp2}-H), 2848 (C_{sp3}–H), 1695 (C=O), 1510, 1498 (C=C Ar), 1269 (C=S); ^{1}H NMR (300 MHz, Acetone-d_6): δ (ppm) 10.58 (1H, s, broad, NH), 8.29 (1H,

s, broad, NH), 7.39-7.41 (d, 2H, *J* = 8.3 Hz, Ar-H), 7.32-7.35 (d, 2H, *J* = 8.3 Hz, Ar-H), 7.19 (s, 2H, Ar-H), 4.13 (q, 1H, *J* = 7.11 Hz, $CHCH_3$), 2.52 (d, 2H, *J* = 7.14 Hz, $(CH_3)_2CHCH_2Ar$), 2.43 (s, 9H, CH_3Ar), 1.82 (m, 1H, $CH(CH_3)_2$), 1.53 (d, 3H, *J* = 7.13 Hz, $ArCHCH_3$), 0.91 (d, 6H, *J* = 6.54 Hz, $CH(CH_3)_2$); ^{13}C NMR (75.5 MHz, Acetone-d_6); 180.2 (C=S), 176.1 (C=O), 140.8, 140.6, 137.5, 132.5, 129.4, 128.1, 127.3, 126.9 (Ar-Cs), 46.1, 44.6, 30.0, 21.7, 21, 18.1 Anal. Calcd. for $C_{20}H_{30}N_2OS$: C, 72.21; H, 7.90; N, 7.32; S, 8.38 found: C, 72.19; H, 7.88; N, 7.30; S, 8.37.

Enzyme assay

Urease inhibition assay

The Jack bean urease activity was determined by measuring amount of ammonia produced with indophenols method described by Weatherburn (28). The reaction mixtures, comprising 20 µL of enzyme (Jack bean urease, 5 U/mL) and 20 µL of compounds in 50 µL buffer (100 mM urea, 0.01 M K_2HPO_4, 1 mM EDTA and 0.01 M LiCl, pH 8.2), were incubated for 30 min at 37 ºC in 96-well plate. Briefly, 50 µL each of phenol reagents (1%, w/v phenol and 0.005%, w/v sodium nitroprusside) and 50 µL of alkali reagent (0.5%, w/v NaOH and 0.1% Sodium hypochloriteNaOCl) were added to each well. The absorbance at 625 nm was measured after 10 min, using a microplate reader (OPTI $_{Max}$, Tunable). All reactions were performed in triplicate. The urease inhibition activities were calculated according to the following formula:

$$\text{Urease inhibition activity (\%)} = (OD_{control} - OD_{sample} \times 100) / OD_{control}$$

Where $OD_{control}$ and OD_{sample} represents the optical densities in the absence and presence of sample, respectively. Thiourea was used as the standard inhibitor for urease.

Free radical scavenging assay

Radical scavenging activity was determined by modifying already reported method (29-30) by 2, 2-diphenyl-1 picrylhydrazyl (DPPH) assay. The assay solution consisted of 100 µL of DPPH (150 µM), 20 µL of increasing concentration of test compounds and the volume was adjusted to 200 µL in each well with DMSO. The reaction mixture was then incubated for 30 minutes at room temperature. Ascorbic acid (Vitamin C) was used as a reference inhibitor. The assay measurements were carried out by using a micro plate reader (OPTI $_{Max}$, Tunable) at 517 nm. The reaction rates were compared and the percent inhibition caused by the

presence of tested inhibitors was calculated. Each concentration was analyzed in three independent experiments run in triplicate.

Cytotoxicity evaluation using brine shrimp assay

Culturing and harvesting of *Artemia salina*

Artemia salina cysts were incubated for hatching in a rectangular dish with a plastic divider with several holes making two uneven compartments. The container was filled with 3.3% solution of artificial sea water and dry yeast sprinkled into the larger compartment which was darkened. The smaller compartment was illuminated with light at 28 °C. After 24 hours, hatched A. salina cysts were transferred to fresh artificial seawater and incubated for a further 24 hours under artificial light and aeriation. The phototropic nauplii were collected by pipette from the lighted compartment.

Brine shrimps assay

A. salina nauplii (20) were counted macroscopically using Pasteur pipette against a lighted background and transferred into each sample vial and the solutions were made to 5mL with test compound using serial dilutions with brine solution. A drop of dry yeast suspension was added as food to each vial. All the vials were maintained under light. The surviving nauplii were counted with the aid of a magnifying glass after 24 hours. The mean mortality at the three dose levels for compound was determined and repeated thrice. Potassium dichromate was used as reference standard. After 24 the LD50 were calculated by Probit analysis.

Kinetic study

Urease inhibition was measured by varying the concentration of urea in the presence of different concentrations of compound **4e** (0.0, 0.025, and 0.01 nM), compound **4h** (0.00, 0.0020, 0.0040 and 0.0080 nM) and compound **4j** (0.00, 0.0025, 0.0050 and 0.01nM.Briefly the urea concentration was changed from 100, 50, 25, 12.5, 6.25, 3.12 mM for urease kinetics studies and remaining procedure was same for all kinetic studies as describes in urease inhibition assay protocol. Maximal initial velocities were determined from initial linear portion of absorbances up to 10 minutes after addition of enzyme at per minute's interval. The inhibition type on the enzyme was assayed by Lineweaver-Burk plot of inverse of velocities (1/V) versus inverse of substrate concentration 1/ [S] mM^{-1}. The EI dissociation constant Ki was determined by secondary plot of 1/V versus inhibitor concentration. The reversible kinetics of the enzyme inhibitoe complex was also determined for different

concentration of compound **4h** versus the enzyme concentration (1.25, 2.5, 5, 10, 20 and 30U/mL. Urease activity was determined by measuring ammonia production using the indophenol method as reported previously (31).The results (change in absorbance per min) were processed by using SoftMaxPro.

Computaional studies

Retrieval of target protein

The crystal structure of Jack bean urease (*Canavaliaensiformis*) was accessed from Protein Data Bank (PDB) (www.rcsb.org) having PDBID 4H9M. The target protein was minimized by employing conjugate gradient algorithm and Amber force field in UCSF Chimera 1.10.1 (32). Furthermore, the Molprobity server (33) and Protparam (34) were utilized to assess the stereo-chemical properties of urease structure. The Ramachandran plot and values (35) were obtained from Molprobity server. The Discovery Studio 4.1 Client (36) , a visualizing tool employed to generate the hydrophobicity graph. The overall protein architecture and statistical percentage values of helices, beta-sheets, coils and turn were retrieved from online server VADAR 1.8 (37) .

Designing of synthesized ligand structures

The synthesized chemical structures were sketched in drawing ACD/ChemSketch tool and minimized by molecular visualizing software UCSF Chimera 1.10.1. The biological properties and drug assessment like drug-likeness values, hydrogen bond acceptors (HBA), and hydrogen bond donors (HBD) were predicted through online tools like Molinspiration (http://www.molinspiration.com/) and Molsoft (http://www.molsoft.com/). The number of HBA and HBD were also confirmed by PubChem (https://pubchem.ncbi.nlm.nih.gov/). Moreover, Lipinski's rule of five was analyzed using Molsoft and Molinspiraion tools. The basic biochemical properties like molar refractivity, density, surface tension and polarizability were generated by ACD/Chemsketch.

Molecular docking simulation

Molecular docking experiment was employed on all the ligands **(4a-j)** against crystal structure of urease by using PyRx docking tool (38). The grid box center values (X=10.22, Y=24.56 and Z=46.18) were adjusted with default exhaustiveness value = 8 to maximize the binding conformational analysis. All the compounds were docked separately against urease with 100 numbers of runs in each docking. The docking complexes were evaluated on lowest binding energy (Kcal/mol) values and structure activity relationship (SAR) analyses. The 3D graphical depictions of all the docking complexes were carried out using Discovery Studio (2.1.0).

Molecular dynamics (MD) simulations assay

The best docked energy (Kcal/mol) valued complexes (**4e** and **4h** ligands-receptor) were selected for MD simulation. To interpret the residual backbone flexibility of these complexes MD simulations were carried out by Groningen Machine for Chemicals Simulations (GROMACS) 4.5.4 package (39) with GROMOS 96 force field (40) .The PRODRG Server (41) was employed to generate ligands topology files. Before minimization, the overall system charge was neutralized by adding ions. The energy minimization (nsteps=50000) was done by steepest descent approach (1000 ps) for each protein-ligand complex. Particle Mesh Ewald (PME) method was employed for energy calculation and for electrostatic and Van der Waals interactions; cut-off distance for the short-range VdW (rvdw) was set to 14 Å, where Coulomb cut-off (r coulomb) and neighbour list (rlist) were fixed at 9 Å (42). It permits the use of the Ewald summation at a computational cost comparable with that of a simple truncation method of 10 Å or less, and the linear constraint solver (LINCS) (43) algorithm was used for covalent bond constraints and the time step was set to 0.002 ps. Furthermore, NVT (44) was performed for 100 ps to equilibrate the system with protein and ligand for constant volume, pressure (1 atm) and temperature (300 K). Finally, a 10 ns molecular dynamics simulation was carried out for all the complexes with nsteps 5000000. The RMSD, RMSF, SASA and Rg analysis were carried out using Xmgrace (http://plasma-gate.weizmann.ac.il/Grace/) and UCSF Chimera 1.10.1 software.

Results and discussion

Synthesis

The synthetic pathway used for the synthesis 1-(2-(4-isobutylphenyl)propanoyl)-3-arylthioureas (**4a-j)** is indicated in scheme 1. Initially 2-(4-Isobutylphenyl)propanoyl chloride **2** was freshly prepared from ibuprofen **1** with the use of thionyl chloride this was then added to a suspension of potassium thiocyanate in anhydrous medium of acetone to yield 2-(4-Isobutylphenyl)propanoyl isothiocyanate **3** as intermediates at 50 ^{o}C for 1.5 h, after cooling at room temperature substituted aromatic anilines in acetone were added and the resulting mixture was refluxed until completion as checked by TLC to obtain thioureas (**4a-j)**.

FT-IR spectra showed sharp absorption peaks at 3233 and 3277 cm^{-1} due to N-H vibration, a peak at 3112 cm^{-1} is due to aromatic stretching and a strong peak at 1680 cm^{-1} corresponds to C=O of an amide. The aromatic stretching frequency bands appear in the range 1600-1550 cm^{-1}. Stretching frequency band at 1258 cm^{-1} confirms C=S (thione) functionality. Vibrational modes at 650-745 cm^{-1} correspond to C-Cl stretching vibrations. The C-H (Sp^3) stretching of alkyl chains appears at around 2850 cm^{-1} respectively. ^{1}H-NMR, showed the most deshieldes broad signal at 12.69 ppm for N-H embedded between C=O and C=S in DMSO-d_6, another broad signal appears at 8.69-8.29 ppm for second N-H of the thiourea. The ^{13}C-NMR showed C=S and C=O signals at 180.2 ppm and 176.1 ppm respectively. The aliphatic and aromatic carbons appear at their respective regions.

Urease inhibition assay

The synthesized target compounds **4a-j** have been screened for their inhibitory effects on the ureases. All of the target compounds exhibited good activity with IC_{50} ranging (0.0081-0.4626 nM) while IC_{50} of thiourea is 18.501 nM. The excellent inhibitory potential was shown by derivatives **4e, 4h and 4j** with IC_{50} 0.0086, 0.0081 and 0.0094 respectively as compared to standard thiourea. In compounds **4e, 4h** the presence of 3-NO_2 and 2,3-DiCl have prime importance in urease inhibitory activity. **4j** with benzyl group also exhibit good activity. Compound **4c** is the least active among the series. The urease inhibition potential of the synthesized compound is presented in Table 1.

Free radical scavenging assay

The synthesized compounds **4a-j** were also evaluated for their radical scavenging activity. Compounds **4b, 4i** and **4j** showed excellent radical scavenging activity as compared to the reference vitamin C. **4i** with 2,4,6-trimethyl substitution showed the higher radical scavenging activity as shown in Table 1.

Brine shrimps assay

The cytotoxic activity of the synthesized compounds was evaluated using brine shrimps assay. Compound **4b** with 4-Br substitution showed the lowest LD50 value among all the series is the most cytotoxic while compound **4g** with 4-SO_2NH_2 showed the highest LD50 value is the least active (Table 2).

Kinetic study

Based on our results we select the most potent compound like **4e**, **4h** and **4j** to determine their inhibition type and inhibition constant on jack bean urease. The potential of these compounds to inhibit free enzyme and enzyme substrate complex was determined in term of EI and ESI constants respectively. The kinetic studies of the enzyme by the Lineweaver-Burk plot of 1/V versus 1/[S] in the presence of different compounds concentrations gave a series of straight lines (Figures1-3). The results of **4e** and **4j** compounds showed that both compounds intersected within the second quadrant (Figures 1 and 3). The analysis showed that 1/Vmax increased with increasing K_m in the presence of increasing concentration of compounds. This behavior of both compound (**4e** and **4j**) indicated that it inhibits urease by two different pathwayscompetitively forming enzymeinhibitor (EI) complex and interrupting enzyme-substrate-inhibitor (ESI) complex in noncompetitive manner. The secondary plots of slope versus concentration of compounds **4e** and **4j** showed EI dissociation constants *Ki* while ESI dissociation constants *Ki′* were shown by secondary plots of intercept versus concentration of compounds. A lower value of *Ki* than *Ki′* pointed out stronger binding between enzyme and compounds **4e**, and **4j** which suggested preferred competitive over noncompetitive manners (Table 3). While in case of compound **4h**, Lineweaver–Burk plot gave family of straight lines, all of which intersected at the same point on the x-axis the analysis showed that 1/*V*max remains the same to a new value while that of Km increase to new value. This behavior

indicated that compound **4h** inhibits Urease competitively to form enzyme inhibitor (EI) complex. Secondary plot of slope against concentration of **4h** showed EI dissociation constant (*Ki*). The results of kinetic constants and inhibition constants are summarized in Table 3.

The inhibitory mechanism of jack bean urease by compounds **4h** with concentrations (0.0, 0.0010, 0.0020, 0.0040 and 0.0080) were investigated. The plots of the remaining enzyme activity versus the concentration of enzyme (30, 20, 10, 5, 2.5 and 1.25 U/mL) at different inhibitor concentrations for the catalysis of urea gave a series of parallel straight lines with the same slopes indicating that the inhibitory effect of **4h** on the urease was irreversible (Figure 2).

Computational studies

Structural assessment of predicted protein

Jack bean urease is a class of hydrolase protein. It contains four domains with variant amino acids numbers.Two adjustable nickel atoms are present in domain four of targeted protein. The presence of these metals in the target protein has a significant in the downstream signaling pathways.Six core metal binding residue (His545, His519, Kcx490, His409, His407 and Asp633) were observed in the active binding pocket of target protein. The graphical depiction of domain architecture within target protein and active region with metal bonded residues is mentioned in Figure 4. The VADAR statistical analysis showed the protein architecture is entailedwith 27% helices, 31% β sheets and 41% coils. Ramachandran plots indicated that 97.5% of residues were present in favored regions. The Ramachandran graph values also depict the accuracy of phi (φ) and psi (ψ) angles among the coordinates of urease protein. The predicted graphs and value showed that 96.4% residues were present in favoredand 99.9% are part of allowed region. The predicted Ramachandran graph and individual domains of targeted protein are mentioned in supplementary data (Fig S1and S2).

The Physiochemical properties of target protein were computed by using ProtParam as mentioned in Table 4. The protein Mw was calculated from linear sequence by the aggregation of average isotopic masses of residues while, theoretical *pI*was measured using pK values of amino acids (45). The literature study justified that proteins were distributed across a wide *pI* range (4.31 to 11.78) (46). The predicted *pI* value 6.05 is comparable with

the standard values which showed the accuracy of predicted structure. Furthermore, extinction coefficient indicates how much light a protein absorbs at a certain wavelength. The predicted value of aliphatic and instability indexeswere also showed the stability and relative volume occupied by aliphatic side chains. The predicted GRAVY value showed the sum of hydropathy values of all amino acids (47). The GRAVY negative value indicates it's more hydrophilic and less hydrophobic behavior. The extinction coefficient, aliphatic index values of targeted protein were calculated from the equations as mentioned in supplementary data (Equations i and ii). Moreover, Grand Average of Hydropathy(GRAVY) calculation principle is also mentioned in supplementary data. All the index calculation equations are mentioned in supplementary data.

Lipinski Rule (RO5) and drug likeness predictions

The RO5 analysis justified that most of synthesized compounds were favored the Lipinski rule.It has been observed that hydrogenbonding affinity is considered as a significant parameter for evaluating the drug permeability. Bakht*et al*., (48) justified that exceeded values of HBA (>10) and HBD (>5) in ligands results in poor permeation in the body. Our chemo-informatics analyses showed that all the designed compounds possess <10 HBA and <5 HBD which may confirm their efficacy and good penetration within the body. The predicted results of polar surface area (PSA) and molar volume of all synthesized compounds were also favored their efficacy. Moreover, their log*P* value were also comparable with standard values <5. However, there are plenty of examples available for RO5 violation amongst the existing drugs (49,50). The drug likeness prediction results showed that 4h was most active drug like compounds which has greater drug score (1.74) compared to other. Our *in-silico* depiction for all the compounds showed results. The predicted chemo-informaticproperty of synthesized compounds is mentioned in Table 5.

Molecular docking and binding energy evaluation of lead structures

Molecular docking study was employedto observe the best fitted conformational position of synthesized compounds **4a-j** against target protein urease. The docked complexes were analyzed on the basis of minimum docking energy values (Kcal/mol). Docking results

justified that compounds **4h** and **4e** exhibited a good binding energy value (-9.70 and -8.90 kcal/mol), respectively, as compared to others compounds. The energy values showed that both compounds bind within the active binding region of target protein with best conformation position. The other compounds such as **4a**, **4d**, **4g** and **4i** were also depicts their significance by good binding energy values (-8.30, -8.40, -8.10 and -8.00 Kcal/mol), respectively. The comparative binding energy analysis reveals that most of compounds were binds to the target molecule with better affinity and have strong therapeutical potential against target protein. The compounds 4his confined at good compatible position in the active region of target protein and showed good correlation results with IC_{50} values. Both computational docking and wet data favors that **4h** predicts good therapeutic potential against target protein. The binding energy values of all the docking complexes and IC_{50} values are mentioned in Figure 5.

Binding pocket analysis of synthesized compounds against urease

The docked complexes were further analyzed on the basis of hydrogen binding interactions. The ligands-protein binding interaction showed that all compounds were confined in the active binding pocket of target protein with different binding poses. The best energy values docked complexes were mentioned in Figure 6. No π-π stacking interactions were observed between compounds and aromatic residues of urease. The **4h**-receptor docked complex reveals the best conformational state with hydrogen/hydrophobic interactions. The unique binding pattern was absorbed in **4h** docking complex. In detail, the structure activity relationship (SAR) study showed that six hydrogen bonds were observed in **4h** docking. The chlorine molecule of benzene ring directly interacts with Ala636 with a bonding distance 2.38 Å. Two hydrogen bonds were observed between carbonyl amino ($-NH_2$) groups moieties of **4h** against His593 having a bonding distance 2.48Åand 2.51Å.respectively. Moreover, the carbonyl oxygen of same compound forms hydrogen bond with His593 at a distance 2.92Å. Similarly, carbonyl methoxy and sulfur functional groups form hydrogen bonds against Asp494 having bonding distance 2.95Å and 2.09Å, respectively. Literature study also justified the significance of these interacted residues in hydrogen bonding which strengthen our docking results (51). The detail binding pattern of all the complexes is mentioned in supplementary data (Table. S1). The comparative binding energy and SAR analysis showed the significance of **4h** compound and may consider as potent inhibitors by targeting jack bean urease. The 3D docking depictions of all other compounds are mentioned in supplementary data figures (Figs S3-S11).

MD simulations analysis

Based on docking energy and IC_{50} results, **4e** and **4h** docking complexes were used evaluate the residual flexibility of receptor molecule. MD simulation study was employed at 10ns by using Gromacs 4.5.4 tool. The Root Mean Square Deviation (RMSD) and Root Mean Square fluctuations (RMSF) graphs were assessed to determine the protein structural behavior in docking. Furthermore, radius of gyration (Rg) and solvent accessible surface area (SASA) (A^2) were also keenly focused to analyze the compactness of target protein. Figure 7 showed the RMSD results of both **4e** and **4h** complexes which interprets the protein residual deviation and fluctuations in 10ns simulation time frame. Initially, both graph lines were displayed an increasing trend from 0-2000 ps. The **4e** complex showed higher fluctuations than the **4h**. At 2000ps time, the RMSD values of **4h** and **4e** were 0.25 and 0.3, respectively. From 2000 to 4000ps the **4h** complex remains stable, while **4e** showed increasing trends of fluctuations at 3000ps and after that showed decreasing fluctuations at 4000ps. Moreover same fluctuations trends were observed from 4000ps to 8000ps. The **4e** graph line was more fluctuated than the **4h** and their RMSD value also increased more than 3. Whereas, the **4h** RMSD value remain stable and showed little fluctuations which favor the stability of docking complex. A little increasing trend was observed from 8000ps to 1000ps in **4h** graph line while **4e** showed downward fluctuations. The comparative analysis justified that **4h** complex simulation graph is more stable throughout the simulation time period as compared to **4e** complex. Figure 8 showed the generated RMSF results of both **4e** and **4h** complexes were showed the C and N-terminal lobes fluctuations of target protein throughout the simulation period. The generated graph showed that N-terminal loop region is much fluctuated. Result depicted that higher peaks in RMSF graph showed the loop conformation and its fluctuations in the simulation time. The comparative RMSF results assured the stability of **4h** against targeted protein throughout the simulation period as compared to **4e**. Both RMSD and RMSF graphs depicts the significance of **4h** over **4e** complex. In MD simulations, the stable behaviors of **4h** docked complex throughout MD trajectories thus increasing the efficacy of docking results.

The compactness of receptor protein was evaluated by Radius of gyration (Rg). The generated results exposed that Rg value is stable at 2.05nm values throughout the simulation time frame 0-10000ps. The Rg time graph showed that residual backbone and folding of receptor protein was steadily stable after binding the inhibitors (Figure 9). The solvent-accessible surface area (SASA) results showed that both complexes co-reside at 205 nm^2 in the simulations graphs (Figure 10).

Conclusions

We have described the synthesis of a novel 1-(2-(4-isobutylphenyl)propanoyl)-3-arylthioureas (**4a-j)** as jack bean urease inhibitors. The title compounds were screened for their Jack bean urease inhibition activity, compounds **4e**, **4h** and **4j** showed IC_{50} values 0.0086nM, 0.0081nM and 0.0094nM respectively. The enzyme inhibitory kinetics of the most potent compounds was also determined and it was observed that compound **4h** inhibit the enzyme competitively while derivatives **4e** and **4j** are the mixed type inhibitors. The compound **4h** reversibly binds the urease enzyme showing *Ki* value 0.0012nM. The *Ki* values calculated for compound **4e** and **4j** are 0.0025nM and 0.003nM respectively. The antioxidant activity resuts showed that compounds **4b**, **4i** and **4j** exhibited excellent radical scavenging potential. The computational molecular docking and molecular dynamic simulation of title compounds was also performed and results showed that the wet lab findings are in good agreement to the dry lab results. Based upon our results it is proposed that compound **4h** may act as a lead candidate to design the clinically useful urease inhibitors.

Conflict of Interest

The authors declare no conflicts of interest in this work.

Figure legends

Figure 1: Lineweaver–Burk plots for inhibition of urease in the presence of Compound **4e**. (a) Concentrations of **4e** were (0.0, 0.025, and 0.01 nM) urea concentrations were 100, 50, 25, 12.5, 6.25, 3.12 mM.
Figure 2: Lineweaver–Burk plots for inhibition of urease in the presence of Compound **4h**. (a) Concentrations of **4h** were (0.00, 0.0020, 0.0040 and 0.0080 nM) urea concentrations were 100, 50, 25, 12.5, 6.25, 3.12 mM.
Figure 3: Lineweaver–Burk plots for inhibition of urease in the presence of Compound **4j**. (a) Concentrations of **4j** were (0.00, 0.0025, 0.0050 and 0.01 nM) urea concentrations were 100, 50, 25, 12.5, 6.25, 3.12 mM.
Figure 4: Crystal structure of jack bean urease with active metal bonded residues.
Figure 5: The graphical depiction of docking energy and IC_{50}values.Thebars showed the docking energy values (Kcal/mol) while dark blue for IC_{50} values (nM), **4h** compound depicts good results among other.
Figure 6: Docking complex of **4h** against jack bean urease. The ligand structure is mentioned in grey color, while the functional moieties such as chlorine, amino, sulfur and oxygen are highlighted in green, deep purple, yellow and red colors, respectively. The targeted protein residues are mentioned in light purple color in wire format. Two nickel atoms are also present in grey color. The black dotted lines represent the hydrogen binding while red labeling justified bond distances in angstrom (Å).
Figure 7: RMSD graphs of **4e** and **4h** docked complexes are mentioned in blue and maroon colors respectively, from 0-10000ps time scale.
Figure 8: RMSF graphs of **4e** and **4h** docked complexes are mentioned in blue and maroon colors respectively, from 0-10000ps time scale.
Figure 9: Radius of gyration (Rg) graphs of **4e** and **4h** docked complexes are mentioned in blue and maroon colors respectively from 0-10000ps time scale.
Figure 10: Solvent Accessible Surface Area (SASA) graph of **4e** and **4h** from 0-10000ps.

Figure legends for Supplementary information

Figure S1: Ramachandran graph of jack bean urease.

Figure S2: Domains of jack bean urease with an architecture.

Figure S3: Docking complex of **4a** against jack bean urease.

Figure S4: Docking complex of **4b** against jack bean urease.

Figure S5: Docking complex of **4c** against jack bean urease.

Figure S6: Docking complex of **4d** against jack bean urease.

Figure S7: Docking complex of **4e** against jack bean urease.

Figure S8: Docking complex of **4f** against jack bean urease.

Figure S9: Docking complex of **4g** against jack bean urease.

Figure S10: Docking complex of **4i** against jack bean urease.

Figure S11: Docking complex of **4j** against jack bean urease.

References

1. Kot M., Karcz W., Zaborska W. (2010) 5-Hydroxy-1,4-naphthoquinone (juglone) and 2-hydroxy-1,4-naphthoquinone (lawsone) influence on jack bean urease activity: elucidation of the difference in inhibition activity. Bioorg Med Chem;38:132-137.

2. Ito Y., Shibata K., Hongo A., Kinoshita M. (1998) Ecabet sodium, a locally acting antiulcer drug, inhibits urease activity of Helicobacter pylori. Eur J Pharm;345:193-198.

3. Sanz-Cobena A., Misselbrook T.H., Arce A., Mingot J.I., Diez J.A., Vallejo A. (2008) An inhibitor of urease activity effectively reduces ammonia emissions from soil treated with urea under Mediterranean conditions. Agric Ecosyst Environ;126:243-249.

4. Allison M.C., Howatson A.G., Torrance C.J., Lee F.D., Russell R.I. (1992) Gastrointestinal damage associated with the use of nonsteroidal antiinflammatory drugs. N Engl J *Med;*327:749-754.

5. McMahon A.D. (2001) Observation and experiment with the efficacy of drugs: a warning example from a cohort of nonsteroidal anti-inflammatory and ulcer-healing drug users. Am J Epidemiol;154:557-562.

6. Rocha G.M., Michea L.F., Peters E.M., Kirby M., Xu Y., Ferguson D.R., Burg M.B. (2001) Direct toxicity of nonsteroidal antiinflammatory drugs for renal medullary cells. Proc Natl Acad Sci;98:5317-5322.

7. Griswold D.E., Adams J.L. (1996) Constitutive cyclooxygenase (COX-1) and inducible cyclooxygenase (COX-2): Rationale for selective inhibition and progress to date. Med Res Rev;16:181-206.

8. Walsangikar S., Bhatia N., Bhatia M. (2013) Structural modification and evaluation of ibuprofen to overcome gi side effects. Int JAPS BMS;2:138-148.

9. Derle D., Gujar K., Sagar B. (2006) Adverse effects associated with the use of nonsteroidal antiinflammatory drugs: An overview. Indian J Pharm Sci;68:409.

10. Omar F.A. (1998) Cyclic amide derivatives as potential prodrugs. Synthesis and evaluation of N-hydroxymethylphthalimide esters of some non-steroidal anti-inflammatory carboxylic acid drugs. Eur J Med Chem;33:123-131.

11. Nagpal D., Singh R., Gairola N., Bodhankar S., Dhaneshwar S.S. (2006) Mutual azo prodrug of 5-aminosalicylic acid for colon targeted drug delivery: synthesis, kinetic studies and pharmacological evaluation. Indian J Pharm Sci;68:171.

12. Sarkate A.P., Lokwani D.K., Patil A.A., Bhandari S.V., Bothara K.G. (2011) Synthesis and evaluation of anti-inflammatory, analgesic, ulcerogenicity and nitric oxide-releasing studies of novel ibuprofen analogs as nonulcerogenic derivatives. Med Chem Res; 20:795-808.

13. Lolli M.L., Cena C., Medana C., Lazzarato L., Morini G., Coruzzi G., Manarini S., Fruttero R., Gasco A. (2001) A new class of ibuprofen derivatives with reduced gastrotoxicity. J Med Chem;44:3463-3468.

14. Koch K.R. (2001) New chemistry with old ligands: *N*-alkyl-and *N*,*N*-dialkyl-*N*′-acyl (aroyl) thioureas in co-ordination, analytical and process chemistry of the platinum group metals. Coordin Chem Rev;216:473-488.

15. Du Y.R., Wang S., Lin J.J., Huang S.M., Zhou, H. (2008) Nonlinear Oxidation of Thiourea in an Unbuffered Medium. *Chin J Chem*;26:1771-1779.

16. Torres V., Rayol V., Magalhães M., Viana G., Aguiar L., Machado S., Orofino H., D'Elia E. (2014) Study of thioureas derivatives synthesized from a green route as corrosion inhibitors for mild steel in HCl solution. Corrosion Sci;79:108-118.

17. (a) Saeed A., Flörke U., Erben M.F. (2014) A review on the chemistry, coordination, structure and biological properties of 1-(acyl/aroyl)-3-(substituted) thioureas. J Sulfur Chem;35:318-355. (b) Saeed A., Qamar R., Fattah T.A., Flörke U., Erben M.F. (2016) Recent developments in chemistry, coordination, structure and biological aspects of 1-(acyl/aroyl)-3-(substituted) thioureas. Res Chem Intermed;43:3053-3093.

18. Arslan H., Duran N., Borekci G., Koray Ozer C., Akbay C. (2009) Antimicrobial activity of some thiourea derivatives and their nickel and copper complexes. Molecules;14:519-527.

19. Saeed S., Rashid N., Jones P.G., Ali M., Hussain R. (2010) Synthesis, characterization and biological evaluation of some thiourea derivatives bearing benzothiazole moiety as potential antimicrobial and anticancer agents. Eur J Med Chem;45:1323-1331.

20. Zhang Y.-M., Wei T.-B., Xian L., Gao L.-M. (2004) An efficient synthesis of polymethylene-bis-aroyl thiourea derivatives under the condition of phase-transfer catalysis. Phosphorus Sulfur and Silicon;179:2007-2013.

21. Vedavathia P., Sekhara K.C., Rajua C.N. (2013) Synthesis, spectral characterization and antimicrobial activity of thiourea/urea derivatives of amlodipine. Der Pharmacia Lett;5: 199-204.

22. Imran S., Taha M., Ismail N.H., Fayyaz S., Khan K.M., Choudhary M.I. (2015) Synthesis, biological evaluation, and docking studies of novel thiourea derivatives of bisindolylmethane as carbonic anhydrase II inhibitor. Bioorg Chem;62:83-93.

23. Zhang Z., Lu S., Sha C., Xu D. (2015) A single thiourea-appended 1, 8-naphthalimide chemosensor for three heavy metal ions: Fe 3+, Pb 2+, and Hg 2+. Sensors and Actuators B: Chem;208:258-266.

24. Daud A.I., Khairul W.M., Mohamed Zuki H., KuBulat K. (2014) Synthesis and characterization of N-(4-Aminophenylethynylbenzonitrile)-N′-(1-naphthoyl) thiourea as single molecular chemosensor for carbon monoxide sensing. J Sulfur Chem;35:691-699.

25. Guang-Yi L., Hong Z., Liu-Yin X., Shuai W., Zheng-He X. (2011) Improving copper flotation recovery from a refractory copper porphyry ore by using ethoxycarbonyl thiourea as a collector. Miner Eng;24:817-824.

26. Zeng R.-S., Zou J.-P., Zhi S.-J., Chen J., Shen Q. (2003) Novel synthesis of 1-aroyl-3-aryl-4-substituted imidazole-2-thiones. Org Lett; 5:1657-1659.

27. Saeed A., Parvez M. (2006) Synthesis, crystal structure of some new 2-(4-methylbenzoylimino)-3-aryl-4-methyl-1, 3-thiazolines. J Heterocyclic Chem;43: 1027-1030.

28. Weatherburn M. (1967) Phenol-hypochlorite reaction for determination of ammonia. Anal Chem;39:971-974.

29. Reddy C.V.K., Sreeramulu D., Raghunath M. (2010) Antioxidant activity of fresh and dry fruits commonly consumed in India. Food Res Int;43:285-288.

30. Ashraf Z., Rafiq M., Seo S.-Y., Babar M.M. (2015) Synthesis, kinetic mechanism and docking studies of vanillin derivatives as inhibitors of mushroom tyrosinase. Bioorg Med Chem;23:5870-5880.

31. Saeed A., Mahmood S.u., Rafiq M., Ashraf Z., Jabeen F., Seo S.Y. (2015) Iminothiazoline-Sulfonamide Hybrids as Jack Bean Urease Inhibitors; Synthesis, Kinetic Mechanism and Computational Molecular Modeling. Chem Biol Drug Des;87:434-443.

32. Pettersen E.F., Goddard T.D., Huang C.C., Couch G.S., Greenblatt D.M. (2004) UCSF Chimera--a visualization system for exploratory research and analysis. J Comput Chem; 25:1605-1612.

33. Chen V.B., Arendall W.B., Headd J.J., Keedy D.A., Immormino R.M. (2010) MolProbity: all-atom structure validation for macromolecular crystallography. Acta Crystallogr D BiolCrystallogr;66:12-21.

34. Gasteiger E., Hoogland C., Gattiker A., Duvaud S., Wilkins M.R., Appel R.D., Bairoch A.; (In) John M. Walker (ed): The Proteomics Protocols Handbook, Humana Press 2005, 571-607.

35. Lovell S.C., Davis I.W., Arendall W.B., de Bakker P.I., Word J.M. (2003) Structure validation by Calpha geometry: phi,psi and Cbeta deviation. Proteins;50:437-450.

36. Studio D, Discovery. "version 2.1." Accelrys: San Diego, CA (2008).

37. Willard L., Ranjan A., Zhang H., Monzavi H., Boyko R.F. (2003) VADAR: a web server for quantitative evaluation of protein structure quality. Nucleic Acids Res;31:3316-3319.

38. Dallakyan S., Olson A.J. (2015) Small-molecule library screening by docking with PyRx. Methods Mol Biol;1263:243-250

39. Pronk S., Pall S., Schulz R., Larsson P., Bjelkmar P. (2013) GROMACS 4.5: a high-throughput and highly parallel open source molecular simulation toolkit. Bioinformatics; 29:845-854.

40. Chiu S.W., Pandit S.A., Scott H.L., Jakobsson E. (2009) An improved united atom force field for simulation of mixed lipid bilayers. J Phys Chem B;113:2748-2763.
41. Schuttelkopf A.W., van Aalten D.M. (2004) PRODRG: a tool for high-throughput crystallography of protein-ligand complexes. ActaCrystallogr D BiolCrystallogr;60: 1355-1363.
42. Wang H., Dommert F., Holm C. (2010) Optimizing working parameters of the smooth particle mesh Ewald algorithm in terms of accuracy and efficiency. J Chem Phys;133: 034117.
43. Amiri S., Sansom M.S., Biggin P.C. (2007) Molecular dynamics studies of AChBP with nicotine and carbamylcholine: the role of water in the binding pocket. Protein Eng Des Sel;20:353-359.
44. Labik S., Smith W.R. (1994) Scaled Particle Theory and the Efficient Calculation of the Chemical-Potential of Hard-Spheres in the Nvt Ensemble. Mol Simul;12:23-31.
45. Jadhav P.B., Yadav A.R., Gore M.G. (2015) Concept of drug likeness in pharmaceutical research. Int J Pharm Biol Sci;6:142-154.
46. Selick H.E., Beresford A.P., Tarbit M.H. (2002) The emerging importance of predictive ADME simulation in drug discovery. Drug Discov Today;7:109-116.
47. Bonnet P. (2012) Is chemical synthetic accessibility computationally predictable for drug and lead-like molecules? A comparative assessment between medicinal and computational chemists. Eur J Med Chem;54:679-689.
48. Bakht M.A., Yar M.S., Abdel-Hamid S.G., Al Qasoumi S.I., Samad A. (2010) Molecular properties prediction, synthesis and antimicrobial activity of some newer oxadiazole derivatives. Eur J Med Chem;45:5862-5869.
49. Tian S., Wang J., Li Y., Li D., Xu L., Hou T. (2015) The application of in silico drug-likeness predictions in pharmaceutical research. Adv Drug Deliv Rev;86:2-10.
50. Clark D.E., Pickett S.D. (2000) Computational methods for the prediction of 'drug-likeness'. Drug Discov Today;5:49-58.
51. Hameed A., Khan K.M., Zehra S.T., Ahmed R., Shafiq Z., Bakht S.M., Yaqub M., Hussain M., de León A.d.l.V., Furtmann N. (2015) Synthesis, biological evaluation and molecular docking of N-phenyl thiosemicarbazones as urease inhibitors. Bioorg Chem; 61:51-57.

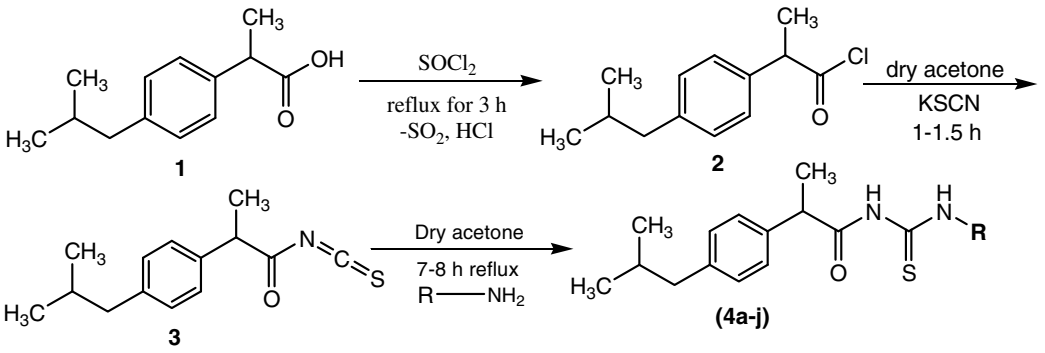

Compound	4a	4b	4c	4d	4e	4f	4g	4h	4i	4j
R	O_2N NO_2	Br	OMe	NO_2 NO_2	NO_2 Cl		SO_2NH_2	Cl Cl	H_3C CH_3 CH_3	

Scheme 1 Synthesis of 1-(2-(4-isobutylphenyl) propanoyl)-3-arylthioureas (**4a-j)**

Table 1: Urease inhibition and free radical scavenging activities of synthesized compounds (4a-j).

Compound	Urease (Jack bean) IC_{50}±SEM (nM)	Free radical % scavenging (100µg/mL)
4a	0.2599±0.00825	30.99±1.32
4b	0.2214±0.00451	69.08±4.46
4c	0.4626±0.022	14.91±0.51
4d	0.1216±0.00451	20.12±0.94
4e	0.0086±0.000167	29.46±1.10
4f	0.0381±0.00214	39.56±1.32
4g	0.0340±0.0020	45.411±2.86
4h	0.0081±0.000351	1.37±0.04
4i	0.0292±0.000981	74.41±4.30
4j	0.0094±0.00040	59.45±3.4
Thiourea	18.501±0.210	------
Vitamin C	----	93.36±5.78

Values are expressed as mean ± SEM
SEM= Standard Error of Mean

Table 2: LD50 of the synthesized compounds (4a-j) using brine shrimp assay.

Compound	Urease (Jack bean) IC_{50}±SEM (nM)
4a	210.15±15.3
4b	209.30±12.2
4c	215.16±16.4
4d	210.88±15.5
4e	234.72±20.12
4f	218.21±18.16
4g	235.15±20.3
4h	225.12±22.14
4i	212.25±18.9
4j	222.18±20.1
Potassium dichromate	0.89±0.01

Table 3: Kinetic parameters of the jack bean urease for urea activity in the presence of different concentration of Ibuprofen derivatives (4a-j)

Code	Dose (nM) (nM)	$1/V_{max}$ (ΔA /Min)	Km (mM)	Inhibition Type	Inhibition	*Ki* (nM)	*Ki′*
	0.00	43.846	2.040				
4e	0.0025	69.230	2.631	Mixed-	----	0.0025	
	0.0044						
	0.01	140.769	3.030	inhibition			
	0.00	154.216	1.11				
4h	0.0020	154.216	4.098	Competitive	Irreversible	0.0012	----
	0.0040	154.216	6.25				
	0.0080	154.216	9.803				
	0.0	84.210	1.063				
4j	0.0025	103.508	2.127	Mixed-	----	0.003	
	0.0147						
	0.0050	128.070	2.941	inhibition			
	0.01	143.859	3.33				

V max = reaction velocity, Km = Michaelis - Menten constant, Ki = EI dissociation constant, Ki′ = ESI dissociation constant, ---- = not calculated

Table 4: Physiochemical properties of predicted structure by ProtParam.

Parameters	Values
Molecular weight (MW)	90747.7 Da
Theoretical *pI*	6.05
Extinction coefficient* (assuming all Cys residues are reduced)	53290
Aliphatic index	90.48
Instability index	31.75
Gran average of hydropathicity (GRAVY)	-0.152

*Extinction Coefficient units $M^{-1}cm^{-1}$ at 280 nm

Table 5: Biological properties of synthesized compounds **4a-j**.

Properties	**4a**	**4b**	**4c**	**4d**	**4e**	**4f**	**4g**	**4h**	**4i**	**4j**
Mw(g/mol)	430	418	370	430	385	374	419	408	354	382
Log*P*	4.10	5.62	4.86	4.22	4.50	5.48	3.59	5.96	4.74	5.73
HBA	6	2	3	6	4	2	5	2	2	2
HBD	2	2	2	2	2	2	4	2	2	2
PSA(A^2)	108	33	40	109	71	33	83	32	34	31
Mol. Vol	401	371	381	400	375	366	396	381	366	412
No. SC	1	1	1	1	1	1	1	1	1	1
Drug Score	0.08	1.23	0.99	0.97	0.51	1.61	1.08	1.74	1.09	1.56